

## Stress Corrosion of Glass

J.S. Jeon\* and D.H. Jeon\*<sup>2</sup>

\*1 Materials Lab., The University of Arizona, Tucson, AZ 85712, U.S.A.

\*2 Corrosion Lab., Korea Maritime University, Pusan, Korea

This paper presents a review of environmentally induced stress corrosion (static fatigue) mechanisms of glass. The rates of extractions of glass constituents by alkali ion-exchange or silica dissolution in water and buffered solution were discussed as a basis of stress corrosion, and the strength increase of abraded glasses after immersing in water was explained in terms of potential strengthening mechanisms. And a detailed chemical bond rupture model in silica glass for the interaction of the environment with mechanically strained bonds at a tip of crack was presented as a stress corrosion crack growth model.

The stress corrosion behavior and static fatigue limit of glasses obtained by measuring crack velocity as a function of applied stress using the double-cantilever cleavage specimen were shown, and the effects of temperature, pH and vapor concentration on fracture behavior and the stages of stress corrosion was also discussed.

### 1. Introduction

Glass is noted for its chemical inertness and general resistance to corrosion, and used as lining, electronic substrate, nuclear waste wrapping and optical fiber waveguide materials, and Table 1 shows compositions of some commercial glasses. But glass is extremely susceptible to stress corrosion cracking(SCC) caused by water or humidity in the environment<sup>(1)</sup>. This failure occurs after being subjected for some time to a stress level too low to cause failure on a short time scale, and is known in the glass literature

as "static fatigue" or "delayed failure". Glass corrosion occurs by two processes (1) selective leaching of the alkali ions, and (2) dissolution of silica network. This corrosion rate is dependent on the glass composition and the environment.

The susceptibility of glass to SCC was observed first by Grenet<sup>(2)</sup>, who noted a time delay to failure and a loading rate dependence of strength. Glass<sup>(3)</sup> is relatively weak when loaded slowly or forced to support the load for a long time. The subsequent studies have demonstrated that the effect is an activated process caused by water in the environment<sup>(4)(5)</sup>. It

Table 1. Some commercial glass composition (%).

Application	SiO <sub>2</sub>	Al <sub>2</sub> O <sub>3</sub>	B <sub>2</sub> O <sub>3</sub>	MgO	CaO	BaO	ZnO	PbO	Na <sub>2</sub> O	K <sub>2</sub> O
Labortary equipment	99.9									
Glassware (pyrex)	80.5	2.2	13						3.8	0.5
Containers	72.2	1.9		1.5	9.6				14.6	
Window glass (soda-lime)	72.0	1.3		3.5	8.2				14.3	
Lamp bulbs	71.5	2.0		2.8	6.6				15.5	1.0
Lead crystal	56.0							29.0	2.0	13.0
Tungsten sealing	75.5	2.6	16.0						3.7	1.7
Sodium vapor resistant	5.5	17.5	16.0		9.51	52.0				
Solder glass	5.0		17.0				14.0	64.0		

is currently believed that static fatigue of glass result from the growth of small pre-existing surface flaws under the combined influence of water vapor and applied load. The small flaws grow until they are large enough to result in catastrophic failure. This decrease in strength with time under load in ambient environments is observed for most glasses and ceramics.

## 2. Corrosion of glass in aqueous solution

The terms "corrosion" and "chemical durability" of glass are often used interchangeably and cover a wide range of situations ranging from invisible surface destruction to gross destruction of glass.

The aqueous corrosion of glasses occurs by two processes<sup>(6)</sup>, (1) the selective leaching of

the alkali ion in the glass or the selective removal of soluble glass constituents by ion exchange which can result in crazing or spalling, and (2) hydrolysis of the Si-O bonds leading to the dissolution of silica network in the glass. And the schematic drawings of glass leaching and dissolution are shown in a Fig. 1.

Hench<sup>(7)(8)</sup> classified the factors affecting glass durability as shown in a Table 2 and revealed the formation of the SiO<sub>2</sub>-rich layer and dissolution of silica on glass after immersing in water by the infrared-reflection spectroscopy<sup>(9)</sup>, and showed decrease of leaching of alkali ion (Na<sup>+</sup>) by adding calcium as a modifier. And to improve the durability of glass, ion exchange technique was applied by exchanging the leachable alkali ion on the surface with a less leachable ion. The example of this technique are proton

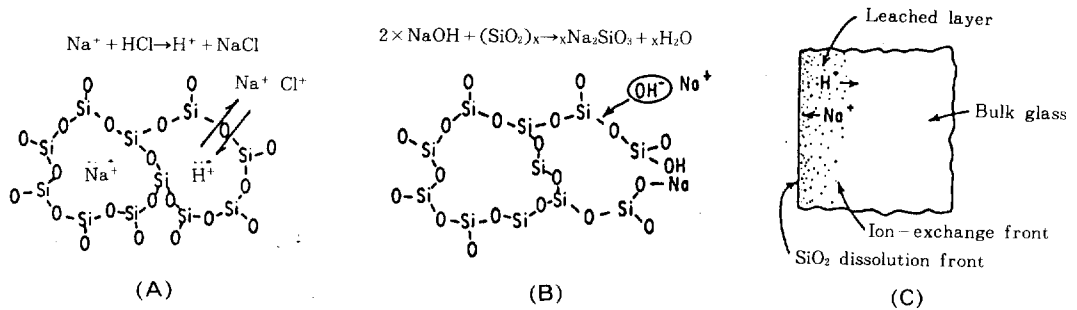


Fig. 1. Schematic drawings<sup>(14)</sup> of (A) leaching, (B) dissolution and (C) reaction zone (much thicker leached layer will develop on a glass of low durability).

Table 2. Factors affecting glass durability.

I. Bulk glass composition
II. Environmental factors
1. Temperature
2. Exposure time (continuous or cycled)
3. Relative humidity
4. Solution pH
5. Presence of inhibitor in the corrosion solution
6. External stresses upon specimen
7. Radiation
8. Solution composition
III. Physical factors
1. Weathering vs. aqueous corrosion
2. Dynamic vs. static corrosion
3. Corrosion behavior of bulk glass vs. powdered glass
IV. Specimen state
1. Thermal history
a. Degree of annealing
b. Phase separation
c. Ratio of crystallization
2. Prior corrosion exposure history
3. Surface roughness and composition
4. Homogeneity of glass
5. Surface treatments

exchange using  $\text{SO}_3$  gas treatment, Cu(I) exchange from CuCl vapor and Li ion exchange in molten  $\text{Li}_2\text{SO}_4$  baths. Bartholomew<sup>(10)</sup> showed that the amount of leached alkali ions were below the detection limit in the  $\text{Na}_2\text{O-SiO}_2$  and  $\text{K}_2\text{O-SiO}_2$  glasses treated with Li containing molten salt baths. And in the case of silica optical fiber, the polymer coating<sup>(11)(12)(13)</sup> were studied to avoid the determinantal effect of moisture on the strength of fiber glass.

### 2.1 Extration of alkali ion in water

Isard<sup>(15)</sup> showed that the amount of alkali ion extracted from a commercial soda-lime-silica glass immersed in water increased linearly with the square root of time. And Doremus<sup>(16)</sup> showed this time dependence of soda-lime-silica glass for times up to 300 hours. In this process, sodium ions diffused to the surface through the glass, and this diffusion was rate controlling process. In general there was a linear relation between the amount of alkali extracted and the square root of time in the early stages of the reaction, but in the later stages, the process became linearly dependent on the time<sup>(17)(18)(19)</sup>. The change from root time depen-

dence to linear variation with time for an alkali glass as shown in a Fig. 2 was explained with the fact that, as the time elapsed, the diffusion velocity would gradually slow down as the leached layer (reaction zone) became thicker because the diffusion distance increase.

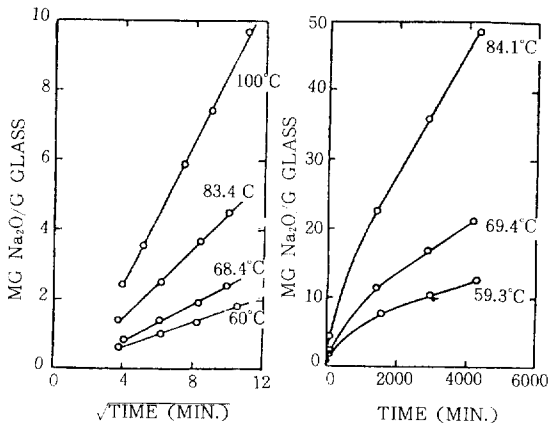


Fig. 2. Water-leaching of  $15\text{Na}_2\text{O}-85\text{SiO}_2$  glass at various temperatures.

## 2.2 Extraction of silica in water

The rate of extraction of silica from binary alkali oxide-silica glasses was related approximately to the rate for alkali so that it may be expressed in terms of following equation<sup>(17)(20)</sup>.

$$Q = Kt^a$$

where  $Q$  is the amount of extracted in time  $t$ , and  $K$  and  $a$  are apparrant constants at constant temperature.

Fig. 3 shows the amount of silica extracted against the time. The value of  $a$  is larger than 1. The value of  $K$  increases as the silica content of the glass decrease. Thus, unlike alkali, silica extracted from a glass decreases as its percentage in the glass increases.

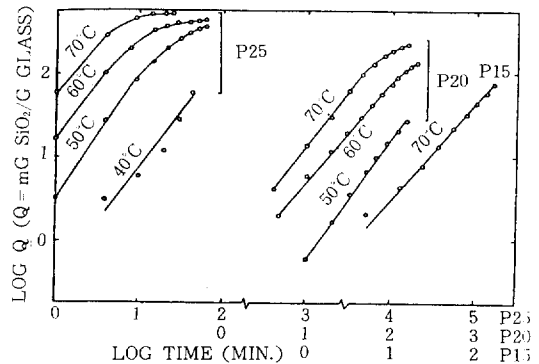


Fig. 3. Time dependence of silica extraction by the water for potassium oxide-silica glasses. (P15:  $15\text{K}_2\text{O}-85\text{SiO}_2$ , P20:  $20\text{K}_2\text{O}-80\text{SiO}_2$ , P25:  $25\text{K}_2\text{O}-75\text{SiO}_2$ )

## 2.3 Extractions of alkali and silica in buffered solution

The pH dependence<sup>(17)(21)</sup> of alkali extraction for all the glasses fell into two regions in binary glasses as well as soda-lime-silica glass; (1) the rate of extraction is almost independent of pH of solution from pH 1 to about 9, and (2) above 9, the rate decreases with increasing pH because the transport of alkali ions through the leached layer is retarded. The amount of alkali extracted against pH change is shown in a Fig. 4. Tholen<sup>(22)</sup> concluded that in the range of pH 4.5 - 9, aqueous corrosion is a combination of a dissolution and diffusion-controlled leaching of alkali ions governed by the penetration of molecular water which independent of composition and pH of the corroding solution, and at a pH of 13, the rate of leaching proceeds much more slowly and the outward diffusion of Na ion becomes rate determining and not the inward diffusion of  $\text{H}_2\text{O}$ . The quantity of silica extracted from a glass<sup>(17)(21)</sup> in a given time increases with pH increasing after pH of about 7 as shown in a Fig. 4.

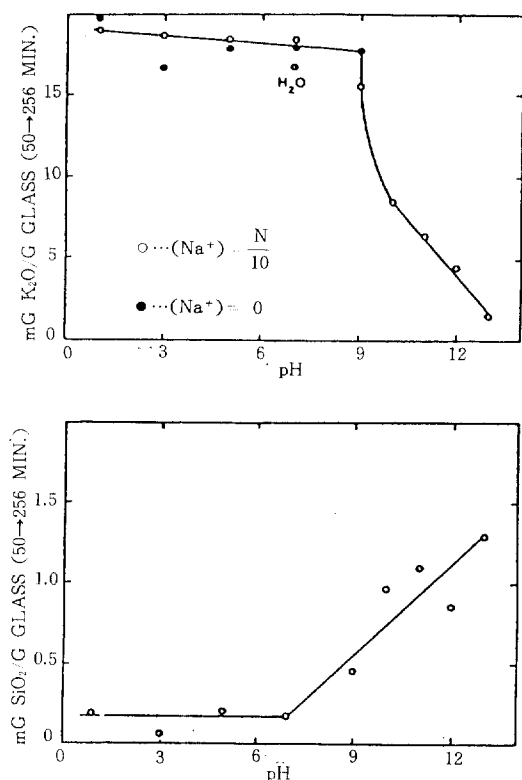
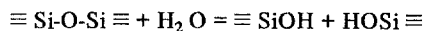


Fig. 4. The pH dependence of alkali and silica extraction at 35°C for 15K<sub>2</sub>O–85SiO<sub>2</sub> glass.

### 3. Crack blunting of glass

When the abraded high-silica rod\* which has surface crack is kept in water, the strength is increased<sup>(23)</sup>. This strength increase is explained by the release of the residual tensile stress assisting the diffusion process around crack tip<sup>(24)(25)</sup>, and the change in the crack tip geometry due to the crack tip blunting<sup>(23)(26)(27)</sup> caused by the dissolution or ion-exchange reaction of the glass in water as following chemical reaction;



\* to avoid alkali-water ion exchange which can produce the surface stress.

The crack blunting increases the ratio of crack-tip curvature as shown in Fig. 5 and 6, and strength is increased because the strength is proportional to curvature inversely. This curvature effect on strength can be explained by Inglis equation;

$$\sigma_{\max} = 2\sigma\sqrt{\frac{c}{\rho}}$$

where  $\sigma_{\max}$  is the maximum stress at tip of crack,  $\sigma$  is the applied stress,  $c$  is the crack length and  $\rho$  is the crack-tip curvature.

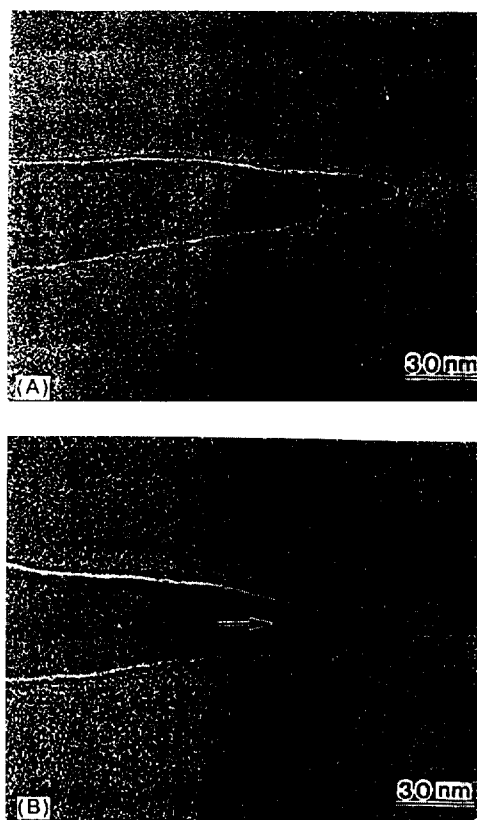


Fig. 5. Blunting of crack tip. (A) immediately after crack introduction and (B) after immersing in water at 90°C for 7 days.

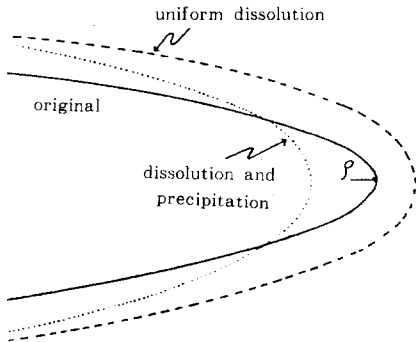


Fig. 6. Schematic drawing of crack-tip geometry.

And Tomozawa<sup>(26)(28)</sup> showed that the increase of strength of high-silica glass immersed in  $H_2O$  and  $Si(OH)_4$  at  $88^\circ C$  for 240 hours are 16% and 20% respectively, and the rate of strength increase by aging in water is the reverse order of chemical durability of glasses with water (i.e., soda-lime glass > borosilicate glass > high-silica glass), and the same order of the ion exchange tendency (i.e., abraded soda-lime glass showed higher rate in acid than alkali), and an acidic solution produced the fastest strengthening.

#### 4. Chemical bond rupture in silica glass

In silica glass, the bridging Si-O-Si bonds connect adjacent  $[SiO_4]^{-4}$  tetrahedral units as shown in a Fig. 7<sup>(29)</sup>. And these bonds support applied stress, therefore its rupture is important in fracture process. The interaction between a strained bridging bond (Si-O-Si) at crack tip in silica and a water molecule from the environment can be represented by a three step process as in a Fig. 8<sup>(30)</sup>. This process explains the reason for crack growth promoted by  $H_2O$  for all silicate glasses.

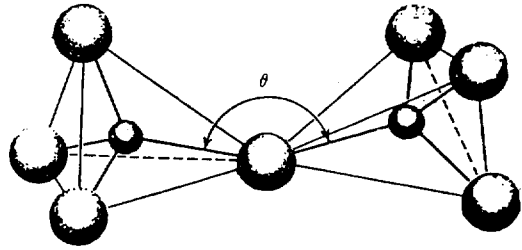


Fig. 7. Schematic drawing of adjacent  $SiO_4$  tetrahedra showing Si-O-Si bond.

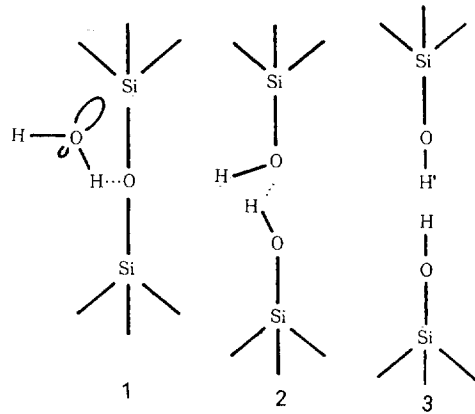


Fig. 8. Representation of proposed reaction between water and strained Si-O-Si bond at crack tip.

- (1) step 1; A water molecule from the environment orients and attaches to a bridging Si-O-Si bond at the strained crack tip. The water molecule is aligned by (a) formation of the hydrogen bond with the O atom in bridging and (b) interaction of the lone-pair orbitals from O atom in water with the Si atom. (Oxygen atom has 2s, 2px, 2py orbitals; two of which sigma bond with hydrogen atoms, one is lone-pair orbitals).
- (2) step 2; A concerted reaction occurs in which proton transfer to the O in bridging is accomplished simultaneously with electron transfer from the O in water to the Si atom. As a result of this reaction, two new bonds are formed one

between O in water and Si, and one between hydrogen and O in bridging, so the original bridging bond between O in bridging and Si is destroyed.

(3) step 3; Rupture of the weak hydrogen bond between O in water and transferred hydrogen occurs to yield surface two Si-O-H group on each fracture surface.

This rupture model predicts that the other environmental molecule which would promote stress-corrosion crack growth in SiO<sub>2</sub> possessed lone pair orbitals available at one portion of the molecule and proton donor sites at the other site such as water. There may be size limitations to fit between the Si-O bond since the Si-O bond distance is only 1.63 Å<sup>(31)</sup>. To evaluate this prediction, crack growth experiments were performed on vitreous silica in water, N<sub>2</sub> gas atmospheres of various low relative humidity, and several nonaqueous environments. Fig. 9 shows the crack growth curves for ammonia

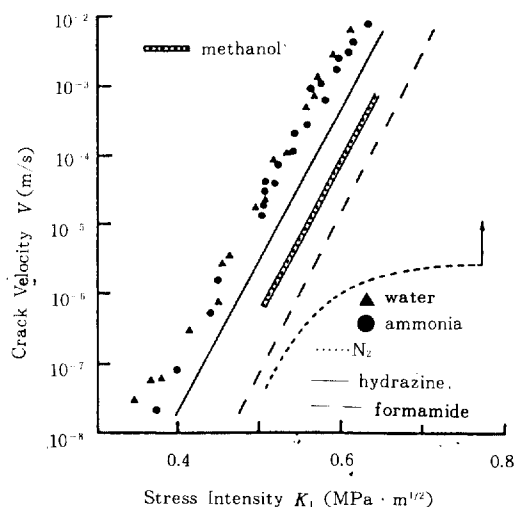


Fig. 9. Fracture behavior of vitreous silica.

(NH<sub>3</sub>), hydrazine (N<sub>2</sub>H<sub>4</sub>), and formamide (CH<sub>3</sub>NO) along with the curves for N<sub>2</sub> gas and water. The absence of a plateau in curves shown in a Fig. 9 for these environment except N<sub>2</sub> gas indicates that they enhance crack growth.

## 5. Stress corrosion behavior of glass

The double-cantilever cleavage specimen<sup>(32)</sup> shown in a Fig. 10 was mounted in a universal testing machine and a constant force was applied to the ends of the specimen after annealing the specimen to remove residual stress and the crack velocity was measured as a function of a applied force in specific environments. The stress intensity factor,  $K_I$  for this configuration specimen can be calculated from following equation<sup>(33)</sup>.

$$K_I = [ PL / ( Wa )^{0.5} t^{1.5} ] ( 3.47 + 2.32t / 2 )$$

Where  $a$  : the uncut portion of glass along the midplane.  $L$ : crack length,  $W$ : thickness,  $2t$ : height,  $P$ : applied force

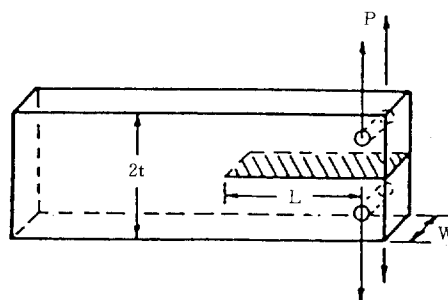


Fig. 10. Specimen configuration. Cross-hatched area designates fracture surface; direction of crack propagation is from right to left.

The fracture behavior of four glasses in water at 25°C is shown in a Fig. 11<sup>(34)</sup>. The composition of glass has a marked effect on the rate of crack growth. For soda-lime silicate and borosilicate glasses, the crack velocity depends exponentially on the stress intensity factor for velocities greater than  $10^{-7}$  and  $10^{-8}$  m/sec respectively. At slower velocities, the crack velocity decreases at greater than an exponential rate, suggesting a threshold stress intensity below which crack motion does not occur. This threshold is known as the static fatigue limit<sup>(35),(38)</sup> (also referred to as stress corrosion limit). The aluminosilicate and silica glasses differ from the others in that there is no indication of static fatigue limit. Charles and Hilling<sup>(37),(38)</sup> explained the fatigue process in terms of balance between the applied stress

which increase the rate of dissolution and surface curvature which slow the chemical dissolution. At stress which the equilibrium between the crack tip dissolution and crack wall dissolution is achieved, crack front maintain constant shape, and the stress below which crack tip radius increases with time is termed as fatigue limit. And Wiederhorn<sup>(39)</sup> and Freiman<sup>(39),(40)</sup> showed the effect of counterion in the test environments on fracture behavior by measuring crack velocity in LiOH solution as a function of  $K_I$ . In Li ion containing solution, the binary soda-silicates glasses showed  $\text{Li}^+\text{-Na}^+$  ion exchange which produce a protective layer and so the rate of crack growth was decreased.

### 5.1 The effect of temperature and pH

The influence of temperature on stress corrosion is shown in a Fig. 12 for soda-lime sili-

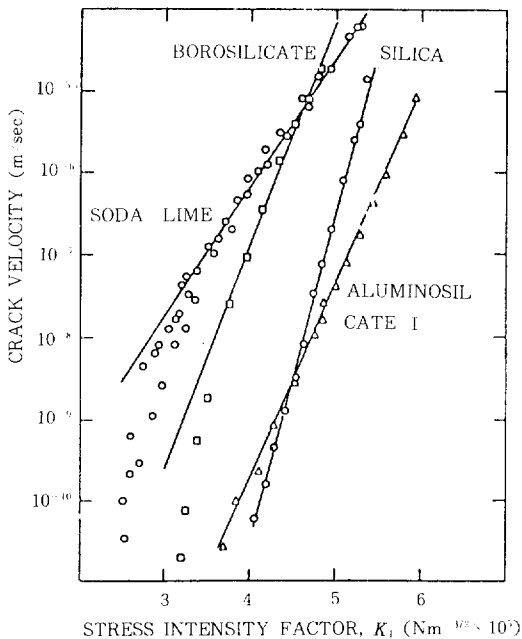


Fig. 11. Fracture behavior of glasses in water 25 C.

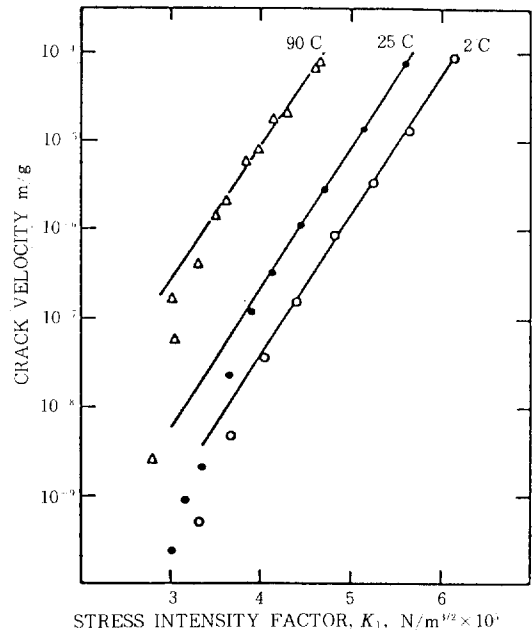


Fig. 12. Influence of temperature on fracture behavior of soda-lime silicate glass in water.

cate glass. The curves showed same slope at different temperatures, but shifted to higher crack velocities with increasing temperature. And the dependence of fracture behavior<sup>(41)</sup> on pH was shown in a Fig. 13. The slope of crack velocity curve is larger in the acidic environment than in the basic environment. This dependence of slope on pH means that the pH affects crack motion and this dependence can be explained by the ionic reaction at crack tip. The reactions between glass and water can produce either acidic or basic solutions at the crack tips by the dynamic balance between the ion-exchange and ion-diffusion processes depending on the composition of the glass. If the glass contains mobile alkali ion, hydration occurs by the ion-exchange between hydrogen ions from the water and alkali ions in the glass, resulting in OH<sup>-</sup> ions in the crack tip solution and the formation of a hydrated silica-rich (an

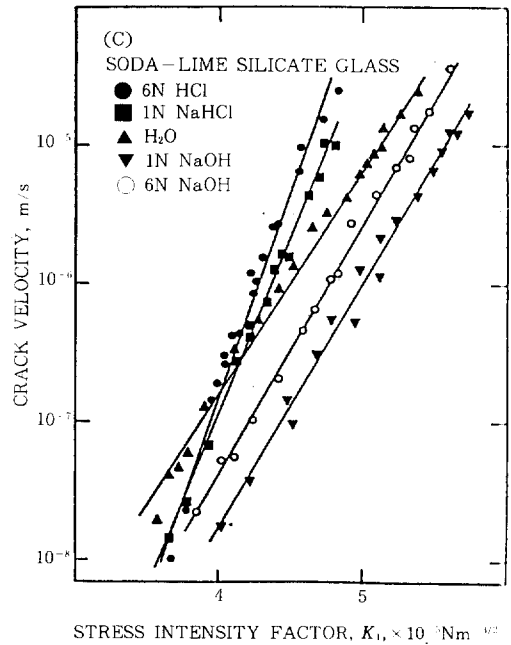
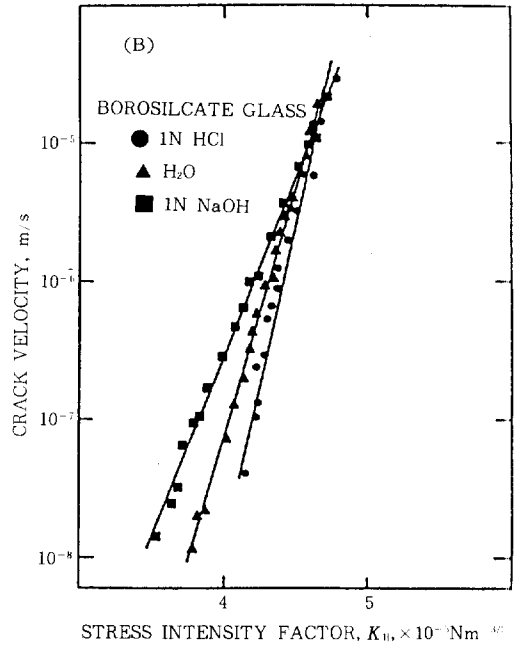
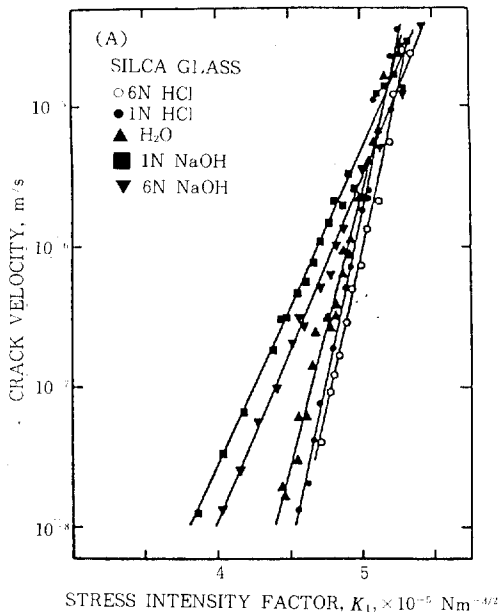
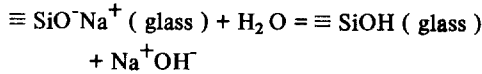


Fig. 13. Fracture behavior of various glasses in acids, bases, and water ; (a) silica glass. (b) borosilicate glass and (c) sodalime silicate glass.

alkali-deficient leached) layer on the surface of glass as the following equation:



And the composition of crack-tip solution can be shown to depend on crack velocity. Mobile ions must diffuse through the glass to reach the interface. Similarly, the counter-diffusion of  $\text{H}^+$  ions through the glass is required for ion-exchange to occur. This sodium-hydrogen ion-exchange can be identified by investigating the strength of glass<sup>(42)</sup>. Metcalfe<sup>(43)(44)</sup> showed modified E-glass fibers containing 5%  $\text{Na}_2\text{O}$  or  $\text{K}_2\text{O}$  fractured spontaneously after immersing in HCl, but the strength was restored by placing it in a NaCl solution. This effect was larger in dilute HCl solution than concentrated HCl solution. And Metcalfe explained the fracture of high-strength fibers ( $4 \times 10^5$  psi) was attributed to flaws or stresses in the surfaces of glass arising from ion-exchange.

## 5.2 Stage in the stress corrosion of glass

The fracture of glass can be divided into two stages; a growth stage in which the crack motion is relatively slow because of chemical attack at crack tip, and a catastrophic stage in which crack motion is rapid when the crack is long enough to satisfy. In a Fig. 14 for the effect of water vapor on crack motion at room temperature, the curves for soda-lime glass are characterized by three distinct regions of crack propagation<sup>(32)(45)</sup>. In region I, the crack velocity,  $V$  is exponentially dependent on the applied force,  $P$  by the following equation;

$$\ln V = a + bp \quad \text{where } a \text{ and } b \text{ are constants.}$$

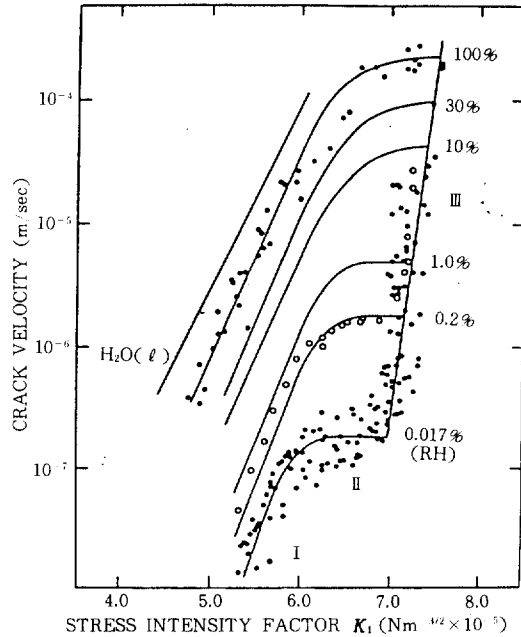


Fig. 14. Dependence of crack velocity on applied force.

And as the relative humidity decreases, the curves shift to lower velocity and higher force. The exponential behaviour of curves and the shift with water concentration can be explained by the Charles-Hilling theory<sup>(37)</sup>. It is believed that crack propagation in the region I is due to corrosive attack of water vapor on the glass at the crack tip. For a given  $K_I$ , crack velocities in the region I were related to the relative humidity, i.e., partial pressure of water through an expression of the form.

$$V = a \left( \frac{P_i}{P_o} \right)^n \exp(bK_I)$$

Where  $a$  and  $b$  are constants,  $P_o$  is the vapor pressure of pure water at temperature of interest, and  $P_i$  is the vapor pressure of water in the gas or the equilibrium vapor pressure over the solution, and  $n$  is the order of the chemical

reaction.

In the region II, the crack velocity is nearly independent of the applied force, but crack velocity is increased as the relative humidity is increased. This behavior can be explained by assuming that the crack velocity is limited by the rate of water vapor transport to the crack tip. As the crack velocity increases the highly strained bonds is increased and the active species depleted zone is increased, thereby creating a diffusion gradient. And the rate of the active species diffusion through the depleted zone to crack tip is becomes slow the crack tip reaction rate, and hence becomes the controlling step in the crack growth process.

In region III, the crack velocity is exponentially dependent on the applied force and is independent of relative humidity in the environment. But for the crack propagation in the region, no satisfactory explanation has been found.

## 6. Summary

1. The aqueous corrosion of glass occurs by the selective leaching of the alkali ion by ion exchange process and dissolution of silica network due to hydrolysis of Si-O bonds.
2. The amount of alkali extracted in water increases with square root of time in the early stage, and increases linearly with time in the later stage. And the rate of alkali extraction decreases with pH above 9, and the rate of silica extraction increases with pH above 7.
3. The crack blunting is explained by the release of the residual stress around crack tip or the change of crack tip geometry by the ion exchange or dissolution.
4. The chemical bond rupture model for silica showed that environments containing molecular structure which has lone pair orbitals and proton donor sites have strong effect on crack growth.
5. The stress corrosion behaviors of glass is dependent on glass composition and environment factors such as temperature, pH and humidity, and three regions were identified. In region I, crack velocity is limited by the rate of corrosive reaction of water with glass at crack tip, and in region II, crack velocity is limited by the rate of transport of water vapor to the crack tip.

## Reference

1. C. J. Phillips, *Amer. Sci.*, 53 (1), 20-51 (1965).
2. Louis Grenet, *Bull. Soc. Eng. Indust. Nat, Paris (Ser. 5)*, 4, 838-848 (1899).
3. J. E. Ritter, Jr., C. L. Sherburne, *J. Am. Ceram. Soc.*, 54 (12), 601-605 (1971).
4. L. H. Milligan, *J. Soc. Glass Technol.*, 13 (52), 351-360T (1929).
5. R. J. Charles, *J. Appl. Phys.*, 29 (11), 1549-1560 (1958)
6. Z. Boksay, G. Bouquet, and S. Dobes, *Phys. Chem. Glasses*, 9 (2), 69 (1968)
7. D. E. Clark, M. F. Dilmore, E. C. Ethridge, and L. L. Hench, *J. Am. Ceram. Soc.*, 59 (1-2), 62-65 (1976).
8. L. L. Hench, *Mat. Res. Soc. Sym. Proc.*, Vol. 125, 189-200 (1988)
9. D. M. Sanders, W. D. Person, and L. L.

- Hench, *Applied spectroscopy*, 28 (3), 247-255 (1974).
10. R. F. Bartholomew, *Ceram. Bull.*, 57 (2), 223-233 (1978)
  11. J. E. Ritter, Jr., *J. Am. Ceram. Soc.*, 56 (7), 402-403 (1973).
  12. T. T. Wang, and H. M. Zupko, *J. Mater. Sci.* 13, 2241-2248 (1978).
  13. H. C. Chandan, and K. Kalish, *J. Am. Ceram. Soc.*, 65 (3), 171-173 (1982).
  14. G. McLellan, and E. Shand, *Glass Engineering Handbook* (3rd Ed.), McGraw-Hill (1984)
  15. R. W. Douglas, and J. O. Isard, *J. Soc. Glass Technol.*, 33 (154), 289-335T (1949).
  16. W. A. Lanford, K. Davis, P. Lamarch, T. Laursen, R. Groleau, and R. H. Doremus, *J. Non-cryst. Solid*, 33, 249 (1979).
  17. R. W. Douglas, and T. M. M. El - Shamy, *J. Am. Ceram. Soc.*, 50 (1), 1 - 8 (1967).
  18. C. R. Das, *Glass Ind.*, 50, 422 - 427 (1969).
  19. Z. Boksay, and G. Bouget, *Phys. Chem. Glasses*, 16 (4), 81-82 (1975).
  20. A. K. Lyle, *J. Am. Ceram. Soc.*, 26 (6), 201-204 (1943)
  21. C. R. Das, *J. Am. Ceram. Soc.*, 63 (3-4), 160-165 (1980).
  22. B.M.J. Smets, and M.G.W. Tholen, *Phys. Chem. Glasses*, 26 (3), 60-63 (1985).
  23. Y. Bando, S. Ito, and M. Tomozawa, *J. Am. Ceram. Soc.*, 67 (3), C36 - C37 (1984).
  24. E. B. Shand, *J. Am. Ceram. Soc.*, 53 (1), 153 (1970).
  25. B. R. Lawn, K. Jakus, and A. G. Gonzales, *J. Am. Ceram. Soc.*, 68 (1), 25-34 (1975).
  26. S. Ito, M. Tomozawa, *J. Am. Ceram. Soc.*, 65 (8), 368-371 (1982).
  27. R. E. Mould, *J. Am. Ceram. Soc.*, 43 (3), 160-167 (1960).
  28. W. T. Han, M. Tomozawa, *J. Am. Ceram. Soc.*, 72 (10), 1837-1843 (1989).
  29. W. D. Kingery, H. K. Bowen, and D. R. Uhlman, *Introduction to Ceramics* (2nd Ed.), 101, Wiley-Interscience (1976).
  30. T. A. Michalske, and S. W. Freiman, *J. Am. Ceram. Soc.*, 66 (4), 284-288 (1983).
  31. T. A. Michalske, and B. C. Bunker, *J. Am. Ceram. Soc.*, 70, 780 (1987).
  32. S. M. Wiederhorn, *J. Am. Ceram. Soc.*, 50 (8), 407-412 (1967)
  33. S. M. Wiederhorn, and L. H. Boiz, *J. Am. Ceram. Soc.*, 53 (10), 543-548 (1970).
  34. S. M. Wiederhorn, A. M. Shorb, and R. L. Moses, *J. Appl. Phys.*, 39 (3), 1569-1572 (1968).
  35. A. J. Holland, and W. E. S. Turner, *J. Soc. Glass Technol*, 24 (101) 46-57T (1940).
  36. E. B. Shand, *J. Am. Ceram. Soc.*, 37 (2) 52-60 (1954).
  37. W. B. Hilling, and R. J. Charles, 682-705, *High strength Materials*, Edited by V. F. Zackay, Wiley, New York (1965).
  38. T. A. Michalske, *Fracture Mechanics of Ceramics*, Vol. 5, 277-290, Plenum Press (1981).
  39. G. S. White, S. W. Freiman, S. M. Wiederhorn, and T. D. Coyle, *J. Am. Ceram. Soc.*, 70 (12), 891-895 (1987)
  40. C. J. Simmons, and S. W. Freiman, *J. Am. Ceram. Soc.*, 64 (11), 683-686 (1981).
  41. S. M. Wiederhorn, and H. Johnson, *J. Am. Ceram. Soc.*, 56 (4), 192-197 (1973).
  42. S. M. Wiederhorn, and H. Johnson, *J. Am. Ceram. Soc.*, 56 (2) 108-109 (1973).

- 
43. A. G. Metcalfe, M. E. Gulden, and G. K. Schmitz, *Glass Technol.*, 12 (1), 15-23 (1971).
44. A. G. Metcalfe, and G. K. Schmitz, *Glass Technol.*, 13 (1), 5-16 (1972).
45. S. M. Wiederhorn, S. W. Freiman, C. T. Simmons and E. R. Fuller, Jr., *J. Mat. Sci.*, 17, 3460-3478 (1982).